



## Supporting Online Material for

### Orbital and Millennial Antarctic Climate Variability over the Past 800,000 Years

J. Jouzel,\* V. Masson-Delmotte, O. Cattani, G. Dreyfus, S. Falourd, G. Hoffmann, B. Minster, J. Nouet, J. M. Barnola, J. Chappellaz, H. Fischer, J. C. Gallet, S. Johnsen, M. Leuenberger, L. Loulergue, D. Luethi, H. Oerter, F. Parrenin, G. Raisbeck, D. Raynaud, A. Schilt, J. Schwander, E. Selmo, R. Souchez, R. Spahni, B. Stauffer, J. P. Steffensen, B. Stenni, T. F. Stocker, J. L. Tison, M. Werner, E. W. Wolff

\*To whom correspondence should be addressed. E-mail: [jean.jouzel@cea.fr](mailto:jean.jouzel@cea.fr)

Published 5 July 2007 on *Science Express*  
DOI: 10.1126/science.1141038

#### **This PDF file includes:**

SOM Text  
Figs. S1 to S8  
References

## Supporting Online Material material

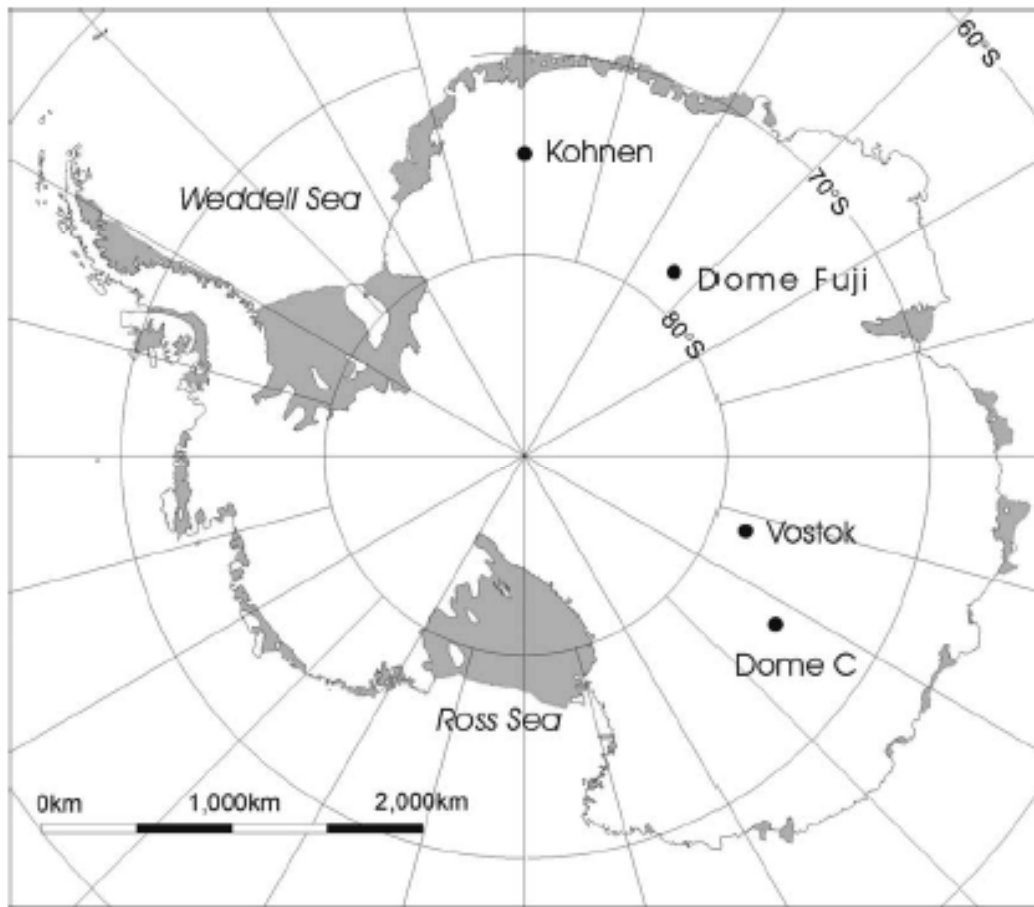


**Figure S1** : Map of deep ice core drillings in East Antarctica

*Drilling* : At EPICA Dome C ( $75^{\circ} 06' S$ ,  $123^{\circ} 21' E$ ), a depth of 3201 m was reached in January 2003. However, due to relatively warm ice ( $-4^{\circ} C$  at 3201m), the drilling team faced difficulties at the end of the field season. Basal temperature is close to the melting point, a situation somewhat similar to that encountered at the Greenland North GRIP site (1). The Dome C drilling - postponed for one season - resumed in November 2004. In order to prevent melting and refreezing of drill chips in the hole and the drill from getting stuck, an ethanol water solution was added at the bottom of the drill hole. This method which had proven successful at North GRIP (1), allowed a final depth of 3260 m to be reached the following month. Drilling was stopped  $\sim 15$  m above the bedrock to prevent

contamination of basal melt water by the drilling fluid (seismic soundings have suggested the presence of melt water just above the bedrock).

**The deuterium profile :** We have completed the deuterium measurements,  $\delta D_{ice}$ , with an optimal accuracy of  $\pm 0.5 \text{ ‰}$  ( $1 \sigma$ ), from the surface down to 3259.7 m, on a continuous and detailed basis of 55 cm along the entire core. Data are available at PANGEA and NCDC data centers.

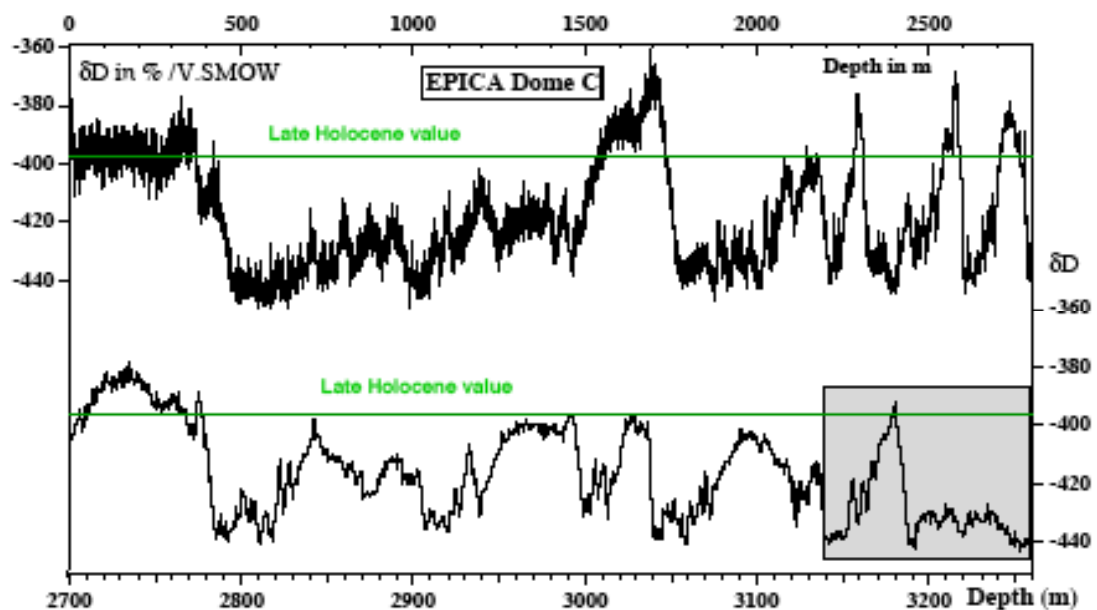


**Figure S2 :** The 55 cm deuterium record as a function of depth in two parts. The extension of the record is highlighted by the grey rectangle. The horizontal lines correspond to the average deuterium value over the last 1000 years (late Holocene).

**The EDC3 timescale :** This improved timescale is constructed in two steps (2, 3). First (2), the same inverse modeling strategy as for EDC2 (4) is used, employing a glaciological dating model which combines an accumulation model and an ice flow model (5) constrained with chronological age markers. Additional time markers used for EDC3 include information derived from air content, which exhibits strong orbital

frequencies (6) and the Matuyama-Brunhes geomagnetic reversal (~ 780 ky BP) as recently identified between 3161 and 3170 m from beryllium 10 measurements (7). In a second step, flow anomalies, resulting in irregularities in the ice thinning function below ~ 2800 m, are accounted for using the precession driven  $\delta^{18}\text{O}_{\text{air}}$  record available between 400 and 800 ky BP to tune this part of the chronology (3). Other notable improvements concern Termination II that was too young in EDC2 (4) and the last 40 ky over which the Antarctic (EDC and EDML) and Greenland ice records are now placed on a common timescale (8, 9, 10).

***The bottom part of the record*** : Figure S3 (left part) shows the new part of the record as a function of depth with corresponding ages indicated on the upper axis using the EDC3 timescale. If undisturbed, this part would cover MIS 20, 21 and 22, but while the oceanic record shows similar amplitudes for MIS 19 and 21, the  $\delta D_{\text{ice}}$  amplitude is three times smaller in this deepest part of the record than just above (Fig.S3). Oxygen 18 measurements performed on this bottom ice show the same low variability. Furthermore, the deuterium-excess profile is very flat and in the range of observed values in shallower ice, which rules out contamination of the ice by the ethanol added to the drilling fluid in the bottom part. Melting and refreezing of the ice can also be dismissed as the air content of the ice is comparable to shallower values. This leads us to suspect that the bottom 60 m of ice have been affected by flow disturbances, a situation previously encountered in Vostok ice below 3310 m (11, 12).

Indeed this lower than expected signal variability is shared by other parameters as illustrated in Fig.S3 by the oxygen 18 of  $\text{O}_2$  in air ( $\delta^{18}\text{O}_{\text{air}}$ ). This parameter depends on continental ice volume, and has been shown to vary coherently with precession over the last four climatic cycles with an amplitude of ~1 ‰ (11, 13). The very low amplitude of  $\delta^{18}\text{O}_{\text{air}}$  before 800 ky BP (~ 0.2 ‰) despite precessional variability and significant

changes in ice-volume (14) argues strongly for the role of a flow disturbance. The same feature is observed for preliminary dust, CH<sub>4</sub> and CO<sub>2</sub> data (not shown). Our suspicion of flow disturbances is also supported by the presence of large particle inclusions. Whether these disturbances are due to stretching of this ice sequence or mixing of layers of different origins will be examined when high-resolution multiparametric records are available.

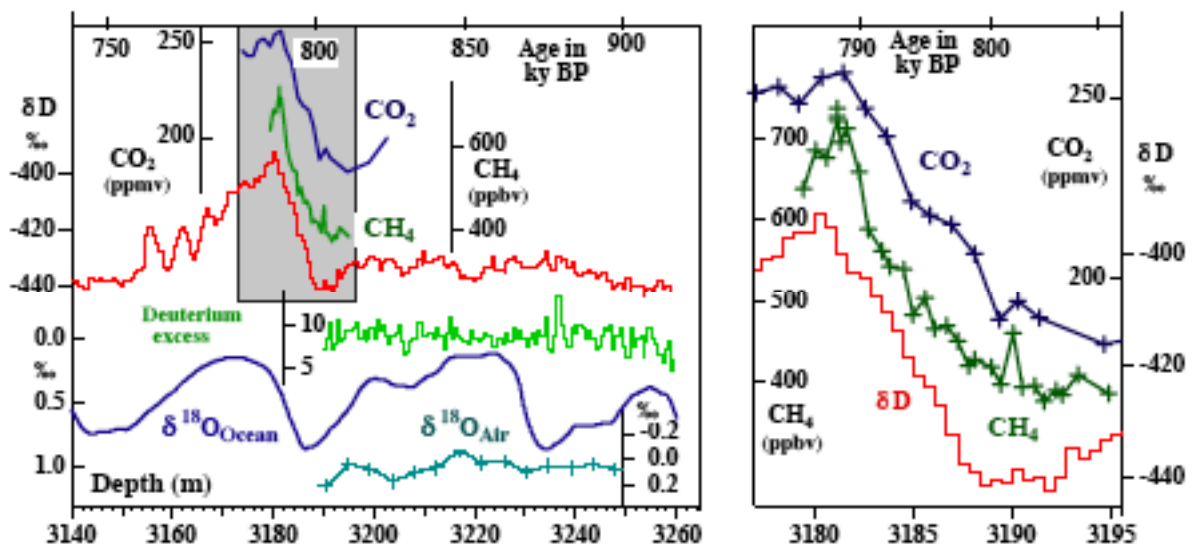


**Figure S3 :** The left part of this graph shows the new part of the record as a function of depth with corresponding ages indicated on the upper axis using the EDC3 timescale. The ice below 3200 m is disturbed and cannot be interpreted climatically (although we still present the hypothetical ages from EDC3). For comparison, the ice sheet  $\delta^{18}\text{O}$  contribution to the deep-sea core record is given as derived by Bintanja et al. (14), plotted against the EDC3 age scale (see upper axis). Additional data include the deuterium excess record ( $\delta^{18}\text{O}$  measured at Copenhagen) and the  $\delta^{18}\text{O}$  in air (measured in Saclay) for depths below 3200 m (older than 827 ky BP), as well as the CO<sub>2</sub> and CH<sub>4</sub> data measured along the transition from MIS 20 to MIS 19 (depth scale). The right part of the graph shows an expanded view of these CO<sub>2</sub> and CH<sub>4</sub> data illustrating the expected depth shifts between these measurements and the ice deuterium record.

In contrast, the stratigraphic continuity of the record above ~3200 m is supported by all available data, especially by preliminary CO<sub>2</sub> and CH<sub>4</sub> measurements performed along the transition between MIS 20.2 and 19 (Fig. S3). In an undisturbed ice record, the changes in atmospheric CO<sub>2</sub> and CH<sub>4</sub> that accompany glacial-interglacial shifts must occur deeper in the ice than the deuterium signature of the temperature change. This is a necessary result of the gas enclosure processes that take place approximately 100 meters below the surface of the ice sheet (15). In contrast, the signatures of a disturbed stratigraphy are abrupt changes in both the deuterium and gas records at the same depth level, as observed in the Vostok ice (11, 12). No such anomaly has been detected at Dome C back to 650 ky BP (16, 17). The CO<sub>2</sub> and CH<sub>4</sub> data obtained on the transition between MIS 20.2 and 19 (Fig.S3) indicate a systematic shift in depth of at least 0.8 m with respect to the deuterium record at the end of the transition (corresponding to the peaks of MIS 19) and suggest a similar or larger shift at the start of the warming corresponding to the end of MIS 20.2. This precludes a depth reversal in the stratigraphic order of the layers. While awaiting the completion of gas measurements above this level, we provisionally assume that this holds true for the entire Dome C record back to MIS 20.2 and that the Dome C core provides a ~ 800 ky old reliable climatic record. As fully discussed by Dreyfus et al. (3), we have however indications from  $\delta^{18}\text{O}_{\text{air}}$  measurements that ice thinning is not regular but with no compromise of the stratigraphy for ice between 800 m (MIS 12) and 3200 m (MIS 20.2), e.g. for the oldest 350 ky of the climatic record.

**Isotopic modeling** : Based on results inferred from simple Rayleigh type models, from existing simulations performed with atmospheric General Circulation Models implemented with water isotopes (IGCM), and from constraints on ice core chronologies and on gas age-ice age difference, it was concluded that at sites such as Vostok and EPICA Dome C, temperature changes are within - 10 % to + 30% of those obtained from

using the spatial  $\delta D$ /temperature slope (18). This result was independently supported by comparison between Byrd and Vostok data (19).

While the above-mentioned IGCM approaches only dealt with two different climates (20, 21), present-day and LGM, numerous time slices (present-day, pre-industrial, 6, 11, 14, 16, LGM and 175 ky BP) are considered for the ECHAM (22) simulations used for deriving the results presented in Figure S4, with corresponding boundary conditions extrapolated from CLIMAP data (23). In the Dome C sector (from the site to coastal Antarctica), the spatial gradients of all time slice calculations are remarkably constant varying by less than  $\pm 0.5\text{‰}/^{\circ}\text{C}$ . The isotopes follow nearly exactly a Rayleigh distillation line in a wide temperature range between roughly  $-20^{\circ}\text{C}$  to  $-70^{\circ}\text{C}$  with isotopic values falling in a very small range for a given temperature, even under very different climate conditions.

This comprehensive modeling approach permits a direct comparison of the spatial slope in a given area with the temporal slope at a given site, allowing us to examine the validity of the isotopic paleothermometer (24). Figure S4 shows the mean isotope ( $\delta D$ ) and surface temperature,  $T_s$ , in the Dome C model grid region plotted against each other. This temporal slope is not only very well defined ( $r^2 = 0.94$ ) but its value ( $6.2\text{‰}/^{\circ}\text{C}$ ) is close to its modern spatial analogue of  $6.04\text{‰}/^{\circ}\text{C}$  (25). This good agreement between spatial and temporal slopes predicted for Dome C fully justifies the conventional temperature interpretation used here and we note that this IGCM modeling approach accounts for changes in origin and seasonality of precipitation. Indeed, the conventional approach leads to amplitudes quite similar to those obtained after correction for changes in source conditions from co-isotopic  $\delta D_{\text{ice}}$  and  $\delta^{18}\text{O}_{\text{ice}}$  determinations performed on our Dome C core over the last 45 ky (26 and therein).

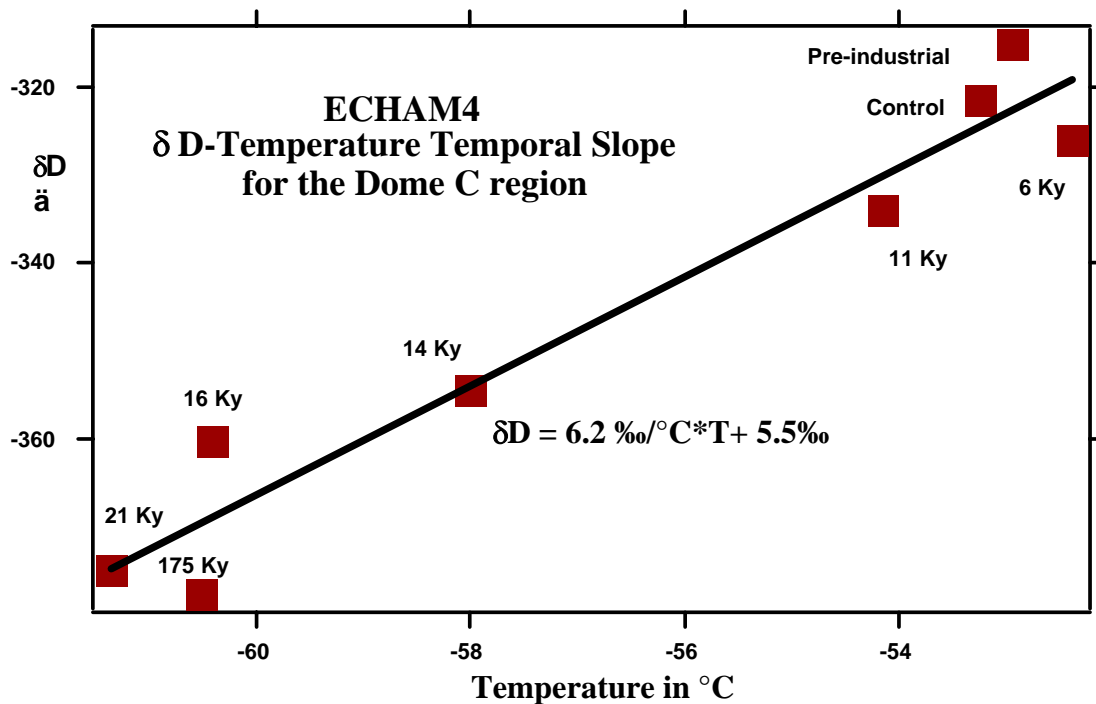


*Figure S4* : Results obtained from a series of new simulations performed using the isotopic version of the ECHAM General Circulation Model. Each square gives the corresponding  $\delta D$  (in ‰ wrt SMOW) and  $T_s$  values for the area corresponding to the Dome C site, with the best fit between these points providing the temporal slope.

The surface temperature change,  $\Delta T_s$  (estimated with respect to the mean value calculated over the last millenium), are calculated using the present-day spatial slope of  $6.04 \text{ ‰/}^\circ\text{C}$  after correction for the change in the isotopic composition of the ocean (13). We thus do not account at this stage of a temperature correction which would result for the change in the source temperature as estimated from co-istopic deuterium and oxygen 18 data (26) which are not yet available for the entire profile. We have also accounted for a slight correction linked with changes in the altitude of the ice sheet as calculated from the glaciological model used to derive the timescale. Typically the elevation decreases by

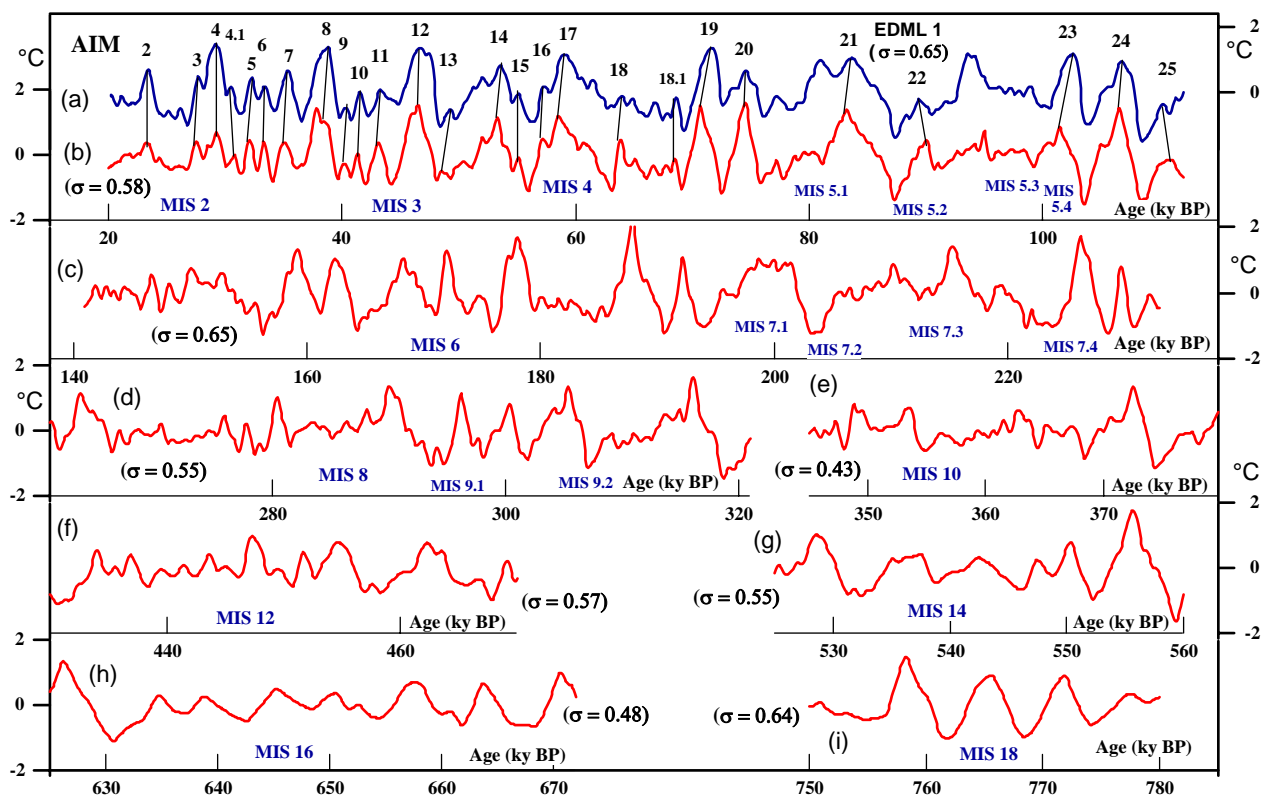


up to ~ 100 m for the coldest glacial periods with a corresponding temperature correction of ~ 1°C.

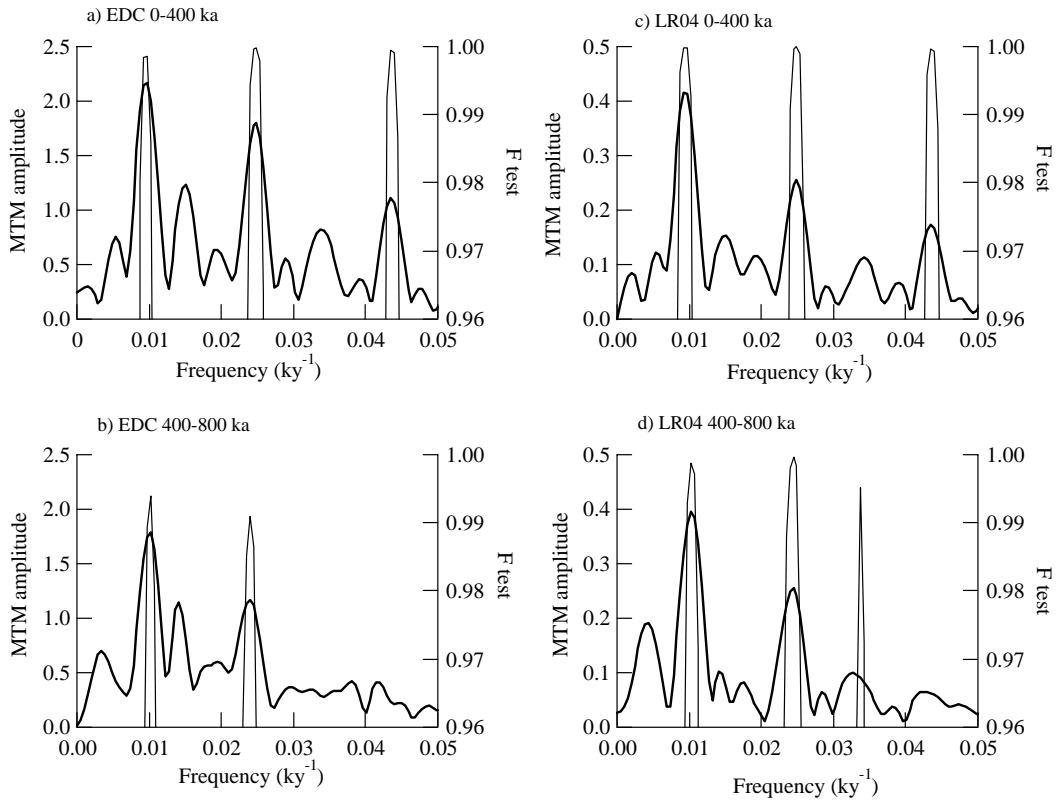
**Millennial events** : The timing between EDC and either North GRIP (Fig. 2) or EDML (Fig. S5) is established using the new common timescale developed for Greenland and Antarctic records. Synchronization between EDC and EDML uses volcanic events, with matching better than 1000 yr back to MIS 5.5 (8), while synchronization between EDML and North GRIP back to 52 ky BP is based on their CH<sub>4</sub> records with estimated uncertainties of ± 400 to ± 800 years largely linked to the gas age / ice age difference (8). In addition, the very detailed <sup>10</sup>Be measurements performed around the peak of production of this cosmogenic isotope ( ~ 40 ky BP) offers the opportunity for a direct and precise (± 200 yr) correlation between Dome C and Greenland records around this event which straddles AIM 10 (27). The temperature changes associated with these millennial Antarctic glacial events have been evaluated after detrending illustrating the succession of large AIM ("A" type event counterparts to long DO events often associated with Heinrich layers) and of smaller AIM that correspond to shorter DO events.

Figure S5 compares the EDC millennial variability with the corresponding variability at EDML (8) during the last glacial period, and at EDC for previous ones. The EDC record exhibits quite similar millennial climate variability during the last 3 glacial periods (Fig. S5) with  $\sigma$  of 0.65 and 0.55 °C during the penultimate and the third glacial periods. We confirm, in particular, the similarity between MIS 3 and MIS 8, previously discussed with the less detailed Vostok  $\delta$ D record (28). The  $\sigma$  value essentially depends on the succession of large AIM, but one can see from Fig. S5 that small AIM are easily identified back to MIS 10. The variability is lower during the previous glacial ( $\sigma = 0.43$  °C for MIS 10) but still high during MIS 12 and MIS 14 ( $\sigma$  of 0.57 °C and 0.55 °C), only slightly lower for MIS 16 ( $\sigma$  of 0.48 °C) and again high for MIS 18 ( $\sigma$  of 0.64 °C).

However, smaller AIM are in any case more difficult to identify during MIS 12, 14, 16 and 18 as a result of lower resolution (one sample from these periods covers 400 to 700 yr). More detailed measurements are required to fully document the millennial variability before Termination V. Available samples will allow the resolution to be improved by a factor of 5.



**Figure S5 :** This graph compares the temperature variability at EDML (curve a) and EDC (curve b) during the last glacial period. Temperature reconstructions have been resampled on a 100 year time step and detrended. We show here the high frequency variability calculated using a 7-point Gaussian filter after detrending. Curves (c) to (i) show the millennial temperature variability at EDC calculated for previous glacial periods using the same algorithm.



**Figure S6** : The power spectra of the  $\Delta T_s$  EDC time series (left) and the Lisiecki and Raymo (25) stacked benthic oxygen 18 record (right) for two time periods : from 0 to 400 ky BP (top) and from 400 to 800 ky BP (bottom). In contrast to the Dome C record, the deep-sea core record has similar relative strength in the obliquity band for the two successive 400 ky periods, the deep-sea core record showing an increase in the amplitude of the obliquity component but only when considering longer time periods (29). These amplitude (continuous curve) and the associated statistical  $F$ -test (thin line) have been calculated with the Multi-Taper Method using the *Analyseries* software (30).

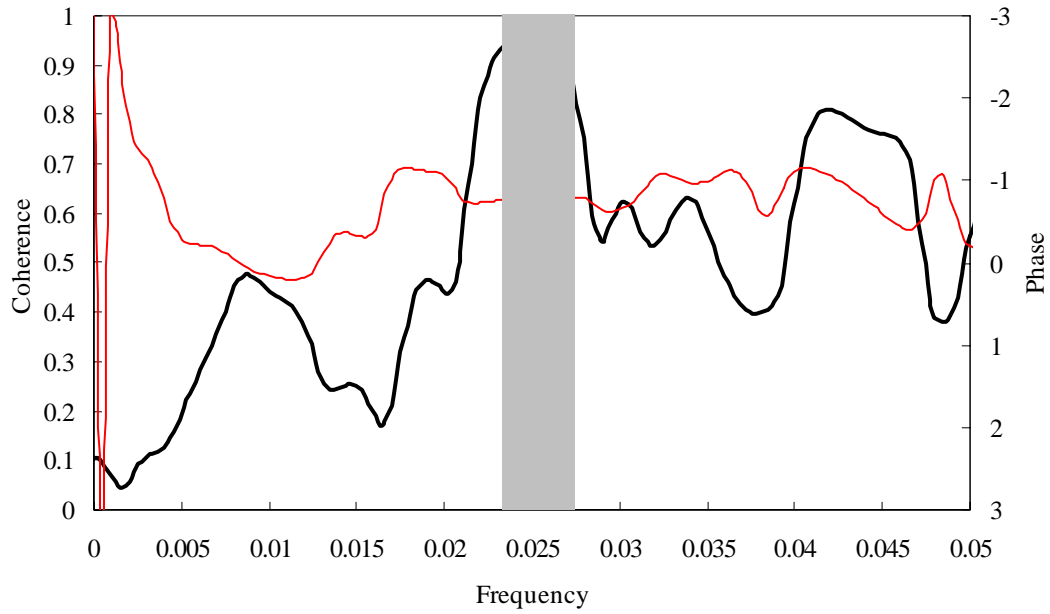


**Figure S7** : Analysis of coherence and phase between EDC temperature and 65°N mid-June insolation performed with the Analyseries software (30): coherence (black, left axis) and lag (radian, red, right axis) versus frequency (in  $\text{ky}^{-1}$ ). The maximum coherence (0.97) is obtained in the obliquity range (grey shaded area) and corresponds to a 5 ky lag of temperature with respect to obliquity. Similar results are obtained when considering the first and second parts of the records (0-400 and 400-800 ka) and when considering obliquity instead of 65°N mid-June insolation.

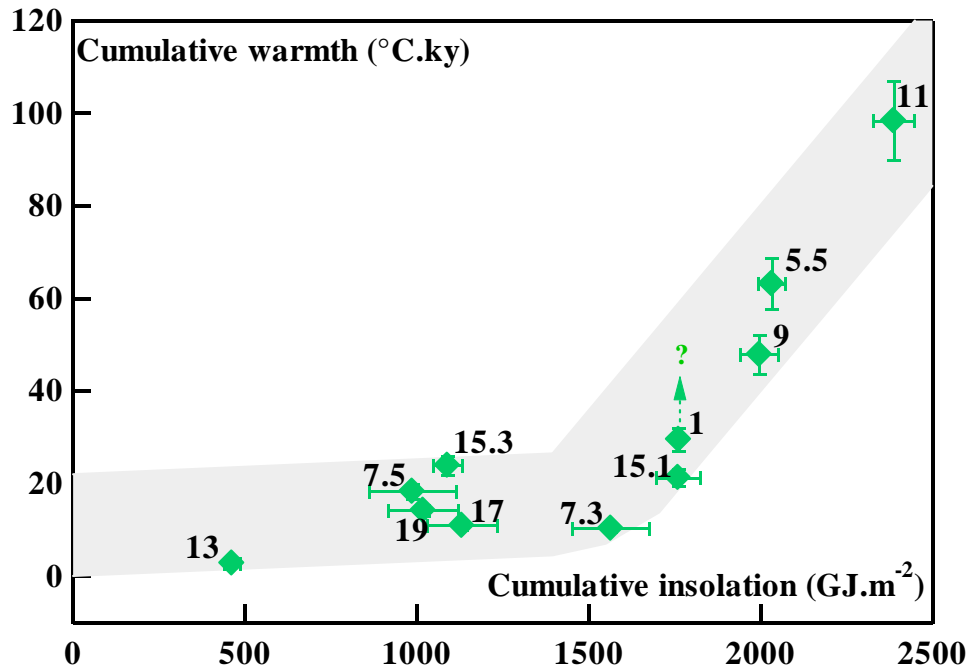


**Figure S8 :** Cumulative warmth ( $^{\circ}\text{C.ky}$ ) calculated as the integral of Dome C temperature reconstruction above a threshold of  $-2.5^{\circ}\text{C}$  (indicated by the horizontal dashed line on Figure 3), represented against cumulative insolation ( $\text{GJ.m}^{-2}$ ), calculated from positive anomalies of centered  $60^{\circ}\text{S}$  annual mean insolation shifted by 5 kyr. Because the current interglacial period, MIS 1, is still ongoing, a vertical dashed arrow indicates the expected direction for MIS 1 total cumulative warmth.

## References

1. North Greenland Ice-core project (NorthGRIP), *Nature*, **431**, 147 (2004).
2. F.Parenin et al, *Climate of the Past Discussions*, **3**, 19 (2007).
3. G.Dreyfus et al., *Climate of the Past Discussions*, **3**, 63 (2007).
4. EPICA Community members, *Nature*, **429**, 623 (2004).
5. F.Parrenin, J.Jouzel, C.Waelbroeck, C.Ritz and J.M.Barnola, *J. Geophys. Res.*, **106**, 31837 (2001).
6. Raynaud, D. et al., *Earth Planet Sci. Lett.*, submitted.

7. G.M.Raisbeck, F.Yiou, O.Cattani & J.Jouzel, *Nature*, **444**, 82 (2006).
8. EPICA Community members, *Nature*, 195, 444 (2006).
9. S.O.Rasmussen et al., *J.Geophys.Res.*, **111**, doi:10.1029/2005JD006079 (2006).
10. K.K.Andersen et al., *Quat.Sci.Rev.*, submitted (2006).
11. J.R. Petit et al. *Nature*, **399**, 429 (1999).
12. D.Raynaud et al. *Nature*, **436**, 39 (2005).
13. M.Bender, *Earth Planet Sci. Lett.*, 204, 275-289 (2002).
14. R.Bintanja, R.S.W van de Wal, R.S.W. & J.Oerlemans, *Nature*, **437**, 125 (2005).
15. J.M.Barnola, P.Pimienta, D.Raynaud & Y.S.Korotkevich, *Tellus*, **43B**, 83 (1991).
16. U.Siegenthaler et al., *Science*, **310**, 1313 (2005).
17. R.Spahni et al., *Science*, **310**, 1317 (2005).
18. J.Jouzel et al., *J.Geophys.Res.*, **108**, doi: 10.1029/2002JD002677 (2003).
19. T.Blunier, J.Schwander, J. Chappellaz, F.Parrenin & J.M.Barnola, *Earth Planet. Sci. Lett.*, **218**, 379 (2004).
20. J.Jouzel, R.D.Koster, R.J.Suozzo & G.L.Russell, *J.Geophys.Res.*, 99, D12, 25791 - 25801, 1994.
21. J.Jouzel, G.Hoffmann, R.Koster & V.Masson, *Quat.Sci.Rev.*, **19**, 363 (2000).
22. G.Hoffmann, M. Werner & M.Heimann, *J.Geophys.Res.*, **103**, 16871, 1998.
23. CLIMAP. *Seasonal reconstructions of the Earth's surface at the last glacial maximum* (Geol. Soc. Am., Boulder, CO, 1981).
24. J.Jouzel et al., *Nature*, **329**, 402(1987).

25. C.Lorius & L.Merlivat in *Isotopes and impurities in snow and ice. Proceedings of the Grenoble Symposium Aug./Sep. 1975* (ed. IAHS) 125, IAHS, Vienna (1977).
26. B.Stenni et al., *Earth Planet. Sci. Lett.*, **217**, 183 (2004).
27. G.M.Raisbeck, F.Yiou, F.& J.Jouzel, *GCA*, **66**, A623 (2002).
28. M.Siddall, T.F. Stocker, T. Blunier, R. Spahni, J.-M. Barnola, and J. Chappellaz, *Paleoceanography*, in press (2006).
29. L.E.Lisiecki & M.E. Raymo, *Paleoceanogr.*, **20**, doi:10.1029/2004PA001071 (2005).
30. D.Paillard, L.Labeyrie & P.Yiou, *EOS, Trans. AGU*, **77**, 379 (1996).